Substrate Specificity, Metal Binding Properties, and Spectroscopic Characterization of the DapE-Encoded *N*-Succinyl-L,L-Diaminopimelic Acid Desuccinylase from *Haemophilus influenzae*[†]

David L. Bienvenue,[‡] Danuta M. Gilner,[‡,§] Ryan S. Davis,[‡] Brian Bennett,[||] and Richard C. Holz*,[‡]

Department of Chemistry and Biochemistry, Utah State University, Logan, Utah 84322-0300, and the National Biomedical EPR Center, Biophysics Research Institute, Medical College of Wisconsin, 8701 Watertown Plank Road, Milwaukee, Wisconsin 53226-0509

ABSTRACT: The catalytic and structural properties of divalent metal ion cofactor binding sites in the *dapE*-encoded *N*-succinyl-L,L-diaminopimelic acid desuccinylase (DapE) from *Haemophilus influenzae* were investigated. Co(II)-substituted DapE enzyme was 25% more active than the Zn(II)-loaded form of the enzyme. Interestingly, Mn(II) can activate DapE, but only to ~20% of the Zn(II)-loaded enzyme. The order of the observed k_{cat} values are Co(II) > Zn(II) > Cd(II) > Mn(II) > Ni(II) ~ Cu(II) ~ Mg(II). DapE was shown to only hydrolyze L,L-*N*-succinyl-diaminopimelic acid (L,L-SDAP) and was inactive toward D,L-, L,D-, and D,D-SDAP. DapE was also inactive toward several acetylated amino acids as well as D,L-succinyl aminopimelate, which differs from the natural substrate, L,L-SDAP, by the absence of the amine group on the amino acid side chain. These data imply that the carboxylate of the succinyl moiety and the amine form important interactions with the active site of DapE. The affinity of DapE for one versus two Zn(II) ions differs by nearly 2.2×10^3 times ($K_{d1} = 0.14\ \mu M$ vs $K_{d2} = 300\ \mu M$). In addition, an Arrhenius plot was constructed from k_{cat} values measured between 16 and 35 °C and was linear over this temperature range. The activation energy for [ZnZn(DapE)] was found to be 31 kJ/mol with the remaining thermodynamic parameters calculated at 25 °C being $\Delta G^{\ddagger} = 64$ kJ/mol, $\Delta H^{\ddagger} = 28.5$ kJ/mol, and $\Delta S^{\ddagger} = -119$ J mol^{-1} K^{-1}. Electronic absorption and EPR spectra of [Co_(DapE)] and [CoCo(DapE)] indicate that the first Co(II) binding site is five-coordinate, while the second site is octahedral. In addition, any spin−spin interaction between the two Co(II) ions in [CoCo(DapE)] is very weak. The kinetic and spectroscopic data presented herein suggest that the DapE from *H. influenzae* has similar divalent metal binding properties to the aminopeptidase from *Aeromonas proteolytica* (AAP), and the observed divalent metal ion binding properties are discussed with respect to their catalytic roles in SDAP hydrolysis.

The importance of identifying novel antibiotic targets is underscored by the emergence of several pathogenic bacterial strains that are resistant to all currently available antibiotics (*1−4*). Most antibiotics work by interfering with vital cellular functions either killing the bacteria or arresting their multiplication (*5*). Currently available antibiotics work on relatively few targets through mechanisms such as inhibiting protein or cell wall synthesis. These targets tend to be conserved among all bacteria and are highly similar in structure and function, such that certain antibiotics kill or inhibit the growth of a broad range of bacterial species (i.e., broad-spectrum antibiotics). Major structural classes of antibiotics include β-lactams, fluoroquinolones, macrolides, tetracyclines, aminoglycosides, glycopeptides, and trimetho-

prim combinations (*3, 6−9*). Since many of the broad spectrum antibiotics are β-lactams, most of the antibiotic discovery effort has centered around new β-lactam containing compounds (*3, 10*). Since any new β-lactam antibiotic will simply be a structural variant of an existing compound and target the same enzymatic pathways, it is likely that any new β-lactam drugs will quickly become useless as bacteria evolve and develop resistance (*3*). To overcome this problem, new enzymatic targets must be identified and novel small molecule inhibitors designed and synthesized to target these enzymes.

A biosynthetic pathway that offers promise for the discovery of novel antibiotic targets is the meso-diaminopimelate (mDAP)/lysine biosynthetic pathway (*3, 11*). Both of the products of this pathway are essential components of the peptidoglycan cell wall for all Gram-negative and most Gram-positive bacteria. Deletion of the gene encoding for one of the enzymes in this pathway, the *dapE*-encoded *N*-succinyl-L,L-diaminopimelic acid desuccinylase (DapE),[1] is lethal to *Helicobacter pylori* and *Mycobacterium smegmatis* (*12, 13*). Therefore, DapEs are essential for cell growth and proliferation and are a part of a biosynthetic pathway
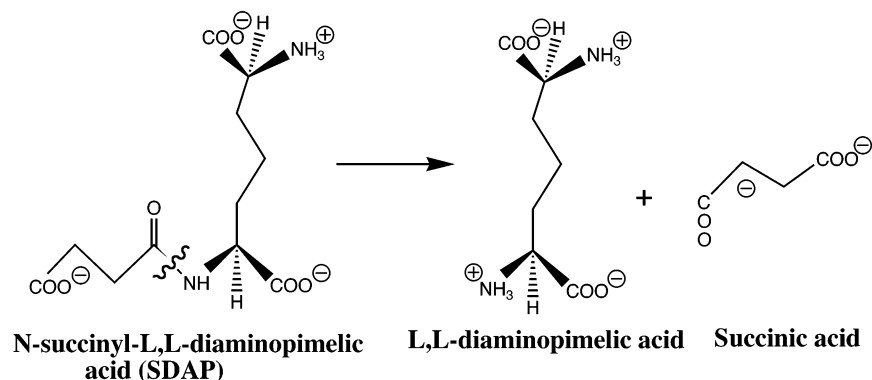
* Address correspondence to the following author. Phone: (435) 797-2609. Fax: (435) 797-3390. E-mail: rholz@cc.usu.edu.
‡ Utah State University.
§ Present address: Department of Chemistry, Silesian Technical University, Poland.
|| Medical College of Wisconsin.

Scheme 1

N-succinyl-L,L-diaminopimelic acid (SDAP) $\longrightarrow$ **L,L-diaminopimelic acid** + **Succinic acid**

that is the only source for lysine in most bacteria. The fact that there are no similar pathways in mammals suggests that inhibitors of enzymes in the mDAP/lysine pathway may provide selective toxicity against bacteria and have little or no effect on humans.

DapEs catalyze the hydrolysis of *N*-succinyl-L,L-diaminopimelic acid (SDAP) (Scheme 1), forming L,L-diaminopimelic acid and succinate (*14*). Native DapEs have been purified from *Escherichia coli* and *Haemophilus influenzae* and have been overexpressed in *E. coli* (*14*, *15*). Both of these DapEs are small, dimeric enzymes (41.6 kDa/subunit) that require two *g*-atoms of zinc per mol of polypeptide for full enzymatic activity. Alignment of all of the known gene sequences for DapE enzymes with the structurally characterized aminopeptidase from *Aeromonas proteolytica* (AAP) and the carboxypeptidase from *Pseudomonas sp* strain-RS-16 (CPG$_2$) (*14*, *16*) indicates that all of the amino acids that function as metal ligands in these enzymes are strictly conserved in DapEs. Similar to AAP, the as-purified DapE enzyme is most active at pH 7.8, contains only one tightly bound Zn(II) ion, exhibits ~80% of its total activity after binding only one Zn(II) ion, and is twice as active after substituting the native Zn(II) ions with Co(II) (*14*).

In an effort to understand the catalytic and structural properties of each divalent metal ion in DapEs, the metal binding properties of the DapE from *H. influenzae* were examined. On the basis of kinetic, electronic absorption, and EPR spectroscopic measurements the substrate specificity, metal binding constants, temperature dependence of the catalytic activity, and the structural/electronic properties of the Zn(II)- and/or Co(II)-loaded DapE enzyme were investigated. These data are discussed in relation to the chemical properties of these metal ions and the known ligand environment of the AAP and CPG$_2$ active sites. Implications of the observed binding properties of these divalent metal ions, with respect to their likely physiological roles in the DapE from *H. influenzae*, are also discussed.

MATERIALS AND METHODS

Reagents. D,L-α,ε-DAP (98% pure), succinic anhydride, and ion-exchange resin (Dowex 50WX8−200, H$^+$ form) were purchased from Sigma. Technically pure 2-naphthalenesulfonic acid (70%) was purchased from Aldrich and crystallized from a 5% aqueous solution of HCl and dried in a vacuum desiccator over CaCl$_2$ to give a white solid of 2-naphthalenesulfonic acid 1-hydrate (confirmed by NMR), Mp 124−125 °C. Microcrystalline cellulose was purchased from EM Science. All solvents and additional chemicals were purchased from either Sigma or Fisher Scientific.

Protein Expression and Purification. The recombinant DapE from *H. influenzae* was expressed and purified, as previously described with minor modifications, from a stock culture kindly provided by Prof. John Blanchard (*14*). Briefly, ~12 g of cell paste were suspended in 50 mL of 10 mM Tricine buffer, pH 7.8, containing four protease inhibitor tablets (complete protease inhibitor tables, Boehringer Mannheim). Lysozyme (10 mg) was added to the mixture and stirred for 30 min at 4 °C. Cells were lysed by sonication (Heat systems-Ultrasonics, Inc.) at 1 min intervals for four repetitions, and the cell debris was removed by centrifugation for 40 min at 12 000*g*. DNase (2 mg) was added, and after ~20 min of incubation, the solution was loaded onto a fast-flow Q-sepharose anion exchange column that had been preequilibrated with 10 mM Tricine, pH 7.8. A flow rate of 3 mL/min was used, and a 600 min linear gradient of NaCl (0.2−0.5 M) was used to elute DapE. DapE activity was detected between 0.25 and 0.3 M NaCl. The active fractions were concentrated using an Amicon YM-10 membrane. Purified DapE from *H. influenzae* exhibited a single band on SDS−PAGE indicating M_r = 41 500. Protein concentrations were determined from the absorbance at 280 nm using a molar absorptivity calculated using the method developed by Gill and Hippel (ϵ_{280} = 36 040 M^{-1} cm^{-1}). The protein concentration determined using this molar absorptivity was in close agreement to that obtained using a Bradford assay. Individual aliquots of purified DapE were stored in liquid nitrogen until needed.

Metal Content Measurements. Apo-DapE was prepared by extensive dialysis for 3 to 4 days against 10 mM EDTA in 50 mM HEPES buffer, pH 7.5. DapE was then exhaustively dialyzed against metal-free (chelexed) 50 mM HEPES buffer, pH 7.5. Any remaining metal ions were estimated by comparing the activity of the apo-enzyme with a sample that had been reconstituted with Zn(II). DapE incubated with

EDTA typically had less than 5% residual activity after dialysis. Enzyme samples used for metal analyses were typically 30 μM. Apo-DapE samples were incubated with ZnCl$_2$ (99.999%; Strem Chemicals, Newburyport, MA) for 30 min prior to exhaustive dialysis into Chelex-treated buffer as previously reported (*17*). Metal analyses were performed using inductively coupled plasma−atomic emission spectrometry (ICP−AES).

Synthesis of N-Succinyl-diaminopimelic Acid (SDAP). The D,D- and L,L-isoforms of DAP were separated from the D,L-isoform using the method described by Bergmann and Stein (*18*). SDAP was synthesized using the procedure described by Lin et al. (*19*) providing an overall yield of 41% (1.84 g; 5.7 mmol); NMR (D$_2$O, 270 MHz), δ (ppm) 1.25−1.45 (m, 2H), 1.55−1.90 (m, 4H), 2.29−2.52 (m, 4H), 3.64 (dd, 1H), 4.05 (dd, 1H), 4.76 (bs, H$_2$O + ammonium ion). The L,L- and D,D-SDAP-isoforms were separated using an HPLC (Shimadzu SCL-10A VP) with a Chirobiotic T column (250 × 10 mm; Alltec). The isocratic mixture of 20% methanol in water (adjusted to pH 4) was used as the eluting solvent. The two isoforms were present in an approximate 1:1 ratio.

Enzymatic Assay of DapE. The specific activity of DapE was determined by monitoring amide bond cleavage of D,D-, L,L-, D,L-, and/or L,D-SDAP at 225 nm in 50 mM HEPES buffer, pH 7.5. The kinetic parameters V_{max} (velocity) and K_m (Michaelis constant) were determined at pH 7.5 by quantifying the amide bond cleavage of L,L-SDAP at 225 nm in triplicate. Enzyme activities are expressed as units/mg where one unit is defined as the amount of enzyme that releases 1 μmol of L,L-SDAP at 30 °C in 1 min. Catalytic activities were determined with an error of ±10%. Initial rates were fit directly to the Michaelis−Menten equation to obtain the catalytic constants K_m and k_{cat}.

Kinetic characterization of DapE with various divalent transition metal ions (Mn(II), Mg(II), Co(II), Ni(II), Cu(II), Zn(II), Cd(II)) in the active site was performed by placing apo-DapE in the presence of 100 μM ultrapure metal (99.999%; Strem Chemicals). After a 1 h incubation period, the activity of metal-substituted DapE was determined by monitoring the hydrolysis of the substrate mixture D,D-, L,L-SDAP. Mixed-metal samples of DapE were prepared by adding 1 equiv of either zinc or cobalt, equilibrating for 30 min, then adding 1 equiv of the second metal ion. The activity of these enzyme samples was determined using the substrate mixture D,D-, L,L-, D,L-, L,D-SDAP.

Spectroscopic Measurements. Electronic absorption spectra were recorded on a Shimadzu UV-3101PC spectrophotometer. All apo-DapE samples used in spectroscopic measurements were made rigorously anaerobic prior to incubation with Co(II) (CoCl$_2$: ≥99.999%; Strem Chemicals, Newburyport, MA) for ∼30 min at 30 °C. All Co(II)-containing samples were handled in an anaerobic glovebox (Ar/5% H$_2$, ≤1 ppm O$_2$; Coy Laboratories) until frozen. Electronic absorption spectra were normalized for the protein concentration, and the absorption was due to uncomplexed Co(II) ($\epsilon_{512\ nm}$ = 6.0 M^{-1} cm^{-1}). Low-temperature EPR spectroscopy was performed using a Bruker ESP-300E spectrometer equipped with an ER 4116 DM dual mode X-band cavity and an Oxford Instruments ESR-900 helium flow cryostat. Background spectra recorded on a buffer sample were aligned with and subtracted from experimental spectra as in earlier work (*20, 21*). EPR spectra were recorded at microwave

R = COO$^-$, CONH$_3^+$,
CH$_2$NHC(NH$_2^+$)NH$_3^+$,
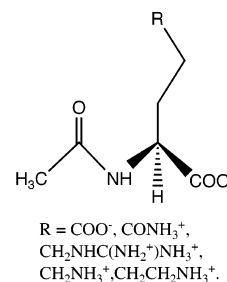CH$_2$NH$_3^+$, CH$_2$CH$_2$NH$_3^+$.

FIGURE 1: Acetylated amino acids.

frequencies of approximately 9.65 GHz: precise microwave frequencies were recorded for individual spectra to ensure precise *g*-alignment. All spectra were recorded at 100 kHz modulation frequency. Other EPR running parameters are specified in the figure legends for individual samples. EPR simulations were carried out using the program XSophe (*22*). Enzyme concentrations for EPR were typically 1−2 mM. DapE was incubated with the appropriate amount of Co(II) for 30 min at 25 °C and then frozen in an EPR tube for analysis.

RESULTS

Analysis of the Zn(II) Content of DapE. The number of tightly bound divalent metal ions per monomer was verified for the DapE from *H. influenzae* by ICP−AES analysis (*14*). DapE samples (30 μM) to which 2−30 equiv of Zn(II) were added were dialyzed extensively at 4 °C with metal-free HEPES buffer. Upon ICP−AES analysis, 1.1 ± 0.1 equiv of zinc were found to be associated with DapE. These data indicate that only one Zn(II) ion is tightly bound to DapE, while the second metal ion is labile on the time scale of the buffer exchange at 4 °C.

Substrate Specificity of DapE. To determine which isomers of SDAP can be hydrolyzed by DapE, we successfully separated the L,D-, D,L-, D,D-, and L,L-isoforms of SDAP using an HPLC (Shimadzu SCL-10A VP) equipped with a Chirobiotic T column (250 × 10 mm; Alltec) (*14*). Hydrolysis experiments performed on each purified isomer of SDAP in the presence of catalytic amounts (6 μM) of Zn-loaded DapE ([ZnZn(DapE)]) indicated that only the L,L-isoform was hydrolyzed by DapE over a 30 min reaction time.

A number of acetylated amino acids were also examined as potential substrates of DapE (*N*-acetyl glutamate; *N*-acetyl glutamine; *N*-acetyl arginine; *N*-acetyl lysine; *N*-acetyl ornithine) (Figure 1). These amino acid derivatives have similar side chains to SDAP and were examined to determine the structural components necessary for substrate binding to the active site of DapE. [ZnZn(DapE)] (6 μM) was unable to hydrolyze any of the acetylated amino acids tested by monitoring amide bond cleavage at 225 nm over the course of 30 min.

Activation of DapE by First Row Transition Metal Ions. Activation of apo-DapE by several first row divalent transition metal ions was examined. Substrate hydrolysis (k_{cat}) of a 1.5 mM D,D-, L,L-SDAP buffered solution was monitored as a function of divalent metal ion concentration under anaerobic conditions (Figure 2). Co(II) provides the most active DapE enzyme and is ∼25% more active than the Zn-(II)-loaded form of DapE (*14*). Interestingly, Mn(II) ions activate DapE but only by ∼20% as compared to Zn(II). The relative ordering of the observed k_{cat} values for D,D-,
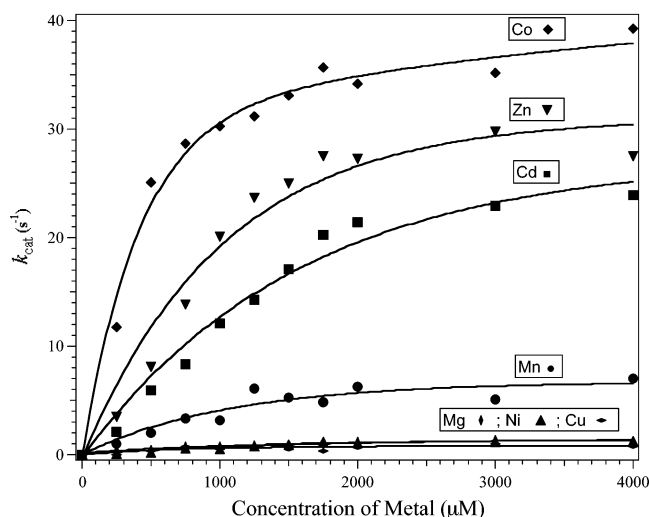
FIGURE 2: Activity of DapE in the presence of various divalent transition metal ions.
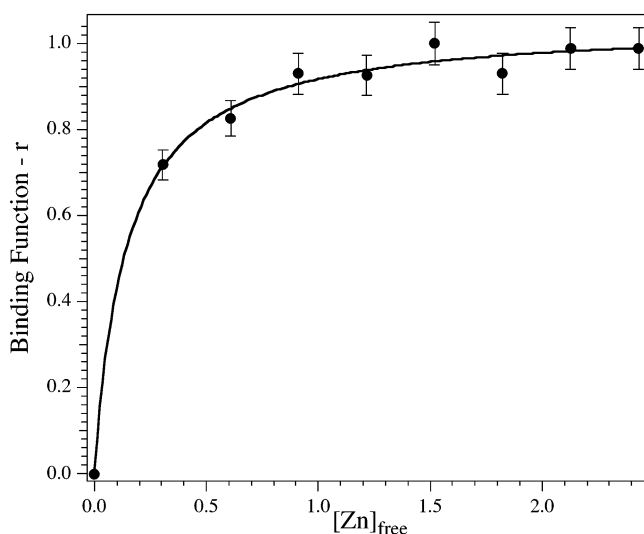

FIGURE 3: Plot of binding function r vs C_s (the concentration of free metal ions in solution) for Zn(II) titration into apo-DapE (50 mM HEPES buffer, pH 7.5).

L,L-SDAP hydrolysis are Co(II) > Zn(II)> Cd(II) > Mn(II) > Ni(II) ∼ Cu(II) ∼ Mg(II). The fact that DapE is active when Cu(II) ions are bound to the active site is very unusual, and to our knowledge there is only a handful of Zn(II) enzymes that can be activated by Cu(II) (*23*).

Titration of Zn(II) into apo-DapE (9 μM) revealed that ∼80% of the catalytic activity could be obtained after the addition of only 1 equiv of metal ion (Figure 3; Table 1). The dissociation constant (K_d) for the first divalent metal binding site was obtained by fitting these titration data to eq 1 (*24*)

$$r = pC_S/(K_d + C_S) \qquad (1)$$

where p is the number of sites for which interaction with Zn(II) is governed by the intrinsic dissociation constant, K_d, and r is the binding function calculated by the conversion of the fractional saturation (f_a) using eq 2.

$$r = f_a p \qquad (2)$$

C_s, the free metal concentration, was calculated using eq 3

$$C_S = C_{TS} - rC_A \qquad (3)$$

where C_{TS} and C_A are the total molar concentrations of metal and enzyme, respectively. A value for K_d was obtained by fitting the data via an iterative process that allowed both K_d and p to vary (Figure 3). The best fits obtained provided a p value of 1 and a K_d value of 0.14 ± 0.05 μM for Zn(II) binding to the first metal binding site in DapE.

Since DapE appears to bind only one divalent metal ion tightly (*14*), we attempted to prepare mixed-metal samples of DapE. One equiv of metal ion, either Co(II) or Zn(II), was incubated with DapE for 30 min followed by the addition of a second equivalent (i.e., Co(II) or Zn(II)). Interestingly, the mono-zinc and mono-cobalt enzymes had activity levels against L,L-SDAP that were ∼80% of those obtained when two metal ions are present (150 vs 180 U/mg for Zn(II) and 170 vs 200 U/mg for Co(II)) (Table 1). However, the mixed-metal samples of DapE (i.e., [ZnCo(DapE)] and [CoZn-(DapE)] had significantly lower specific activities (110 vs 130 U/mg for ZnCo and CoZn, respectively) and K_m values (260 and 740 μM for [ZnCo(DapE)] and [CoZn(DapE)], respectively, vs 730 and 990 μM for [ZnZn(DapE)] and [CoCo(DapE)], respectively). The combination of these data with k_{cat} values for [ZnZn(DapE)] and [CoCo(DapE)] provides the catalytic efficiency (k_{cat}/K_m) that is 11 400 ± 200 and 9000 ± 200 mM^{-1} min^{-1}, respectively. The catalytic efficiency of the [Zn_(DapE)], [Co_(DapE)], [ZnCo(DapE)], and [CoZn(DapE)] enzymes are 6600 ± 200, 7200 ± 200, 16 800 ± 200, and 7200 ± 200 mM^{-1} min^{-1}.

Temperature Dependence of DapE Catalyzed Hydrolysis of L,L-*SDAP*. The thermal stability of DapE was examined in 50 mM HEPES, pH 7.5 buffer. DapE is not particularly thermally stable; therefore, the hydrolysis of L,L-SDAP was only measured between 16 and 35 °C. The specific activity for L,L-SDAP hydrolysis catalyzed by [ZnZn(DapE)] was found to increase with increasing temperature. In a simple rapid equilibrium, $V_{max}/[E] = k_p$, the first-order rate constant. Since the enzyme concentration was not altered over the course of the experiment, an Arrhenius plot can be constructed by plotting ln k_{cat} versus $1/T$ (Figure 4). A linear plot was obtained, indicating that the rate-limiting step does not change as the temperature is increased (*25*). From the slope of the line, the activation energy, E_a, for temperatures between 289 and 308 K was calculated to be 31 ± 2 kJ/mol [ZnZn(DapE)]. Since the slope of an Arrhenius plot is equal to $-E_{a1}/R$ where $R = 8.3145$ J K^{-1} mol^{-1}, other thermodynamic parameters were calculated by the following relations: $\Delta G^{\ddagger} = -RT \ln(k_{cat}h/k_BT)$, $\Delta H^{\ddagger} = E_a - RT$, $\Delta S^{\ddagger} = (\Delta H^{\ddagger} - \Delta G^{\ddagger})/T$, where k_B, h, and R are the Boltzmann, Planck, and gas constants, respectively. The enthalpy and entropy of activation were calculated to be 28.5 kJ/mol and −119 J/(mol K), respectively. The free energy of activation at 25 °C was calculated to be 64 kJ/mol.

Spectroscopic Characterization of [Co_(DapE)] and [Co-Co(DapE)]. The binding of Co(II) to DapE was investigated by electronic absorption spectroscopy since the position and molar absorptivities of Co(II) d−d bands reflect the coordination number and geometry of the metal ions (*26*). UV−vis spectra were recorded at 25 °C using enzyme concentrations of 1 mM. All spectra were recorded under strict anaerobic conditions, and the absorbance for apo-DapE was

Table 1: Kinetic Constants for Zn(II)- and Co(II)-Loaded DapE for L,L-SDAP at 30 °C and pH 7.5

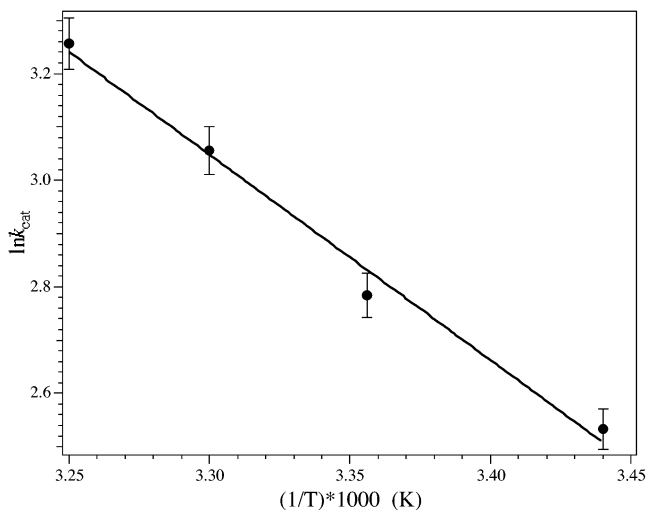| kinetic constants	Zn	ZnZn[a]	Co	CoCo[a]	ZnCo	CoZn
K_m (μM)	730 ± 15	730 ± 15	990 ± 15	990 ± 15	260	740
k_{cat} (s^{-1})	80 ± 5	140 ± 10	120 ± 10	150 ± 10	75 ± 5	90 ± 5
k_{cat}/K_m (mM^{-1} min^{-1})	6600 ± 200	11400 ± 200	7200 ± 200	9000 ± 200	16800 ± 200	7200 ± 200
SA (U/mg)	150 ± 15	180 ± 18	170 ± 17	200 ± 20	130 ± 12	110 ± 11

[a] Measured with 4 equiv of divalent metal ion present.

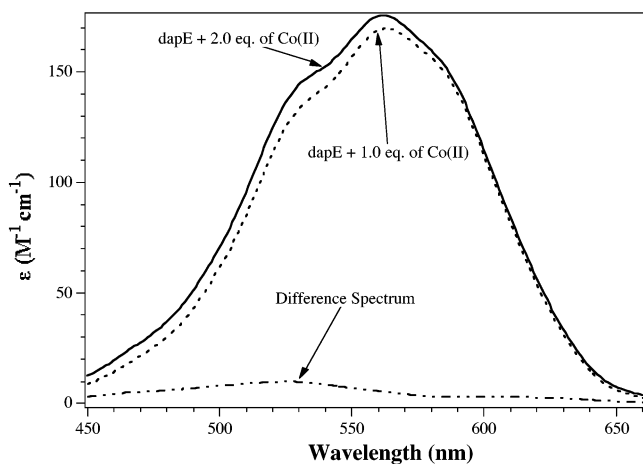FIGURE 4: Arrhenius plot for the DapE catalyzed hydrolysis of L,L-SDAP.

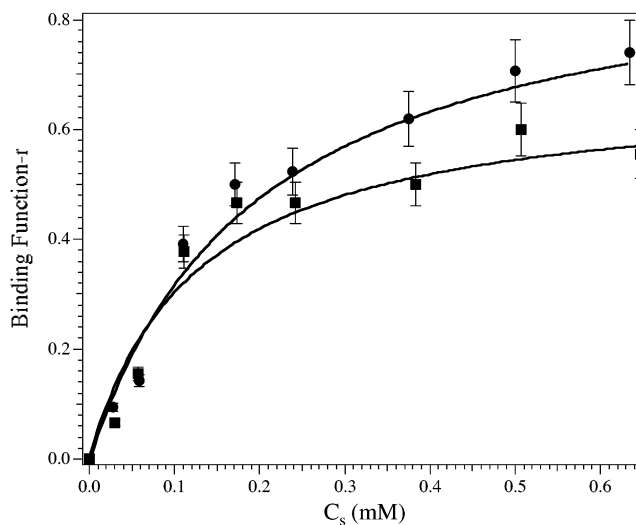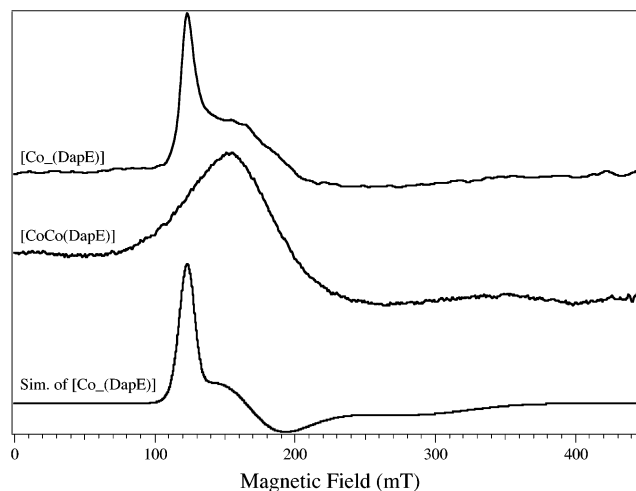FIGURE 5: UV−vis spectra of Co(II)-substituted DapE at pH 7.5.

FIGURE 6: Plot of binding function r vs C_s (the concentration of free metal ions in solution) for the molar absorptivities at 562 nm (solid circles) and 532 nm (solid squares) for a 65 μM DapE sample in 50 mM HEPES buffer, pH 7.5.

FIGURE 7: EPR spectra of Co(II)-substituted DapE at 4 K in 50 mM HEPES buffer pH 7.5.

subtracted. The addition of 1 equiv of Co(II) to DapE (50 mM HEPES buffer, pH 7.5) provided a visible absorption spectrum with bands at 562 nm (ϵ_{562} ~170 M^{-1} cm^{-1}) and shoulders at 530 nm (ϵ_{530} ~130 M^{-1} cm^{-1}) and 575 nm (ϵ_{576} ~150 M^{-1} cm^{-1}) (Figure 5). Addition of a second equivalent of Co(II) increased the absorption intensities at 530 nm to ~140 M^{-1} cm^{-1} but increased the absorbance at 562 nm only ~10 M^{-1} cm^{-1}. The addition of more than 2 equiv slightly increased the absorbance at 562 nm from 180 to 185 M^{-1} cm^{-1} indicative of the presence of [Co(H$_2$O)$_6$] that has a molar absorptivity of ~6 M^{-1} cm^{-1}.

The Co(II) binding properties of DapE were also investigated using electronic absorption spectroscopy by titrating Co(II) into apo-DapE (65 μM) and monitoring the absorption at 530 and 562 nm. Under these conditions, the first equivalent of Co(II) would be tightly bound assuming its binding constant is similar to that of Zn(II). The K_d value for the second divalent metal binding site was then obtained

by fitting the electronic absorption data to eq 1 via an iterative process that allowed both K_d and p to vary after subtraction of the absorption due to the first metal binding site (Figure 6). The best fits obtained provided a p value of 1 and an average K_d value of 300 ± 100 μM.

EPR spectra of [Co_(DapE)] and [CoCo(DapE)] were recorded at several temperatures (3.5−70 K) and microwave powers (0.5−50 mW). EPR spectra of [Co_(DapE)] and [CoCo(DapE)] are presented in Figure 7. Upon addition of 0.25−1.0 equiv of Co(II) to apo-DapE, a signal appeared that was characterized by a sharp feature at $g_{eff} = 5.6$ and a broad underlying feature with a turning point at $g_{eff} = 3.7$. Continued EPR absorption out to 380 mT suggested an unresolved feature centered on a third principal g_{eff} value.

The spectrum was simulated as a single species with an isotropic g factor using the spin Hamiltonian $H = SDS + \beta BgS$ where $S = 3/2$, $g_{\text{real(iso)}} = 2.38$, $D \gg h\nu$, and $E/D = 0.1$. This corresponds to an $M_S = |\pm 1/2\rangle$ ground-state transition, expected for five- or six-coordinate Co(II). A g-strain model for the line widths was employed that assumed $\delta g/g$ values of 0.045, 0.140, and 0.140 for the high-field, middle, and low-field lines, respectively. This apparent anisotropy in g-strain suggests that a contribution to the line shapes may actually be due to strain in the rhombic zero-field splitting parameter, E/D. Because the high-field line in the experimental spectrum was not resolved, an isotropic g-factor ($g_{\text{real(iso)}}$) was assumed, and the same g-strain value as for the middle line was used; no attempt to refine the fit to the high-field absorption was made. Further complications arise from the appearance of passage effects in the experimental spectrum under the experimental conditions employed. Spectra were recorded between 4 and 20 K over a range of microwave powers, and the conditions employed for the spectrum presented represented the best compromise between the effects of rapid passage (worse at higher powers and lower temperatures), relaxation broadening (seen at higher temperatures), and a need to observe adequate signal-to-noise (very poor at low powers). Nevertheless, despite these challenges, the simulation reproduces the experimental spectrum well.

Although the g-factor and rhombic distortion of the axial zero-field splitting observed in the EPR spectrum of [Co_-(DapE)] are typical for species in the related enzyme AAP, the spectrum of DapE exhibits no resolved [59]Co hyperfine splitting (hfs). These data suggest a marked difference in the degrees of collinearity of the effective **g**- and **A**-tensors. An alternative explanation would be the presence of an electron-withdrawing moiety coordinated to the Co(II) ion. Several Cys residues exist in the amino acid sequence of DapE, and the possibility that one or more cysteine-derived sulfur atoms are ligands was explored. Electronic absorption spectrophotometry provided no evidence for S → Co(II) ligand−metal charge-transfer bands in the 300−350 nm region, suggesting that Cys is not a ligand to the Co(II) ion (*26*). In addition, both [ZnZn(DapE)] and apo-DapE were incubated with *N*-ethylmaleimide, a known thiol-modifying reagent, and the remaining activity levels toward L,L-SDAP were determined. For [ZnZn(DapE)], no loss in specific activity was observed. Moreover, reconstitution of apo-DapE with Zn(II) after treatment with *N*-ethylmaleimide provided a fully active enzyme. Therefore, while the precise geometrical factors that give rise to a lack of hfs in the low-field line remain unclear, sulfur coordination of Co(II) is not one of those factors.

The EPR spectrum of [CoCo(DapE)] is similar to spectra observed in AAP, the methionyl aminopeptidase from *E. coli* (*Ec*MetAP), and somewhat similar to $[\text{Co(H}_2\text{O})_6]^{2+}$ (*20*, *21*, *27*). These spectra typically exhibit E/D values of ~0.1, and despite the quite different appearances of the spectra of [Co_-(DapE)] and [CoCo(DapE)], the spin Hamiltonian parameters actually indicate very little change in the degree of axial electronic symmetry for the first Co(II) ion upon binding of a second Co(II) ion. It is difficult to deconvolute the determinants of the line shape of such broad, poorly resolved spectra as that from [CoCo(DapE)], and earlier simulations of AAP and *Ec*MetAP assumed an explicit strain in g_{eff} rather than an attempt to identify the underlying mechanism. Strains
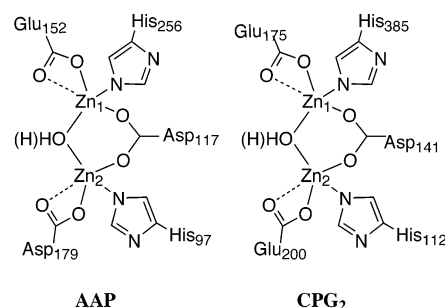

AAP   **CPG$_2$**

FIGURE 8: Active site drawings of AAP and CPG$_2$.

in g and the zero-field splitting parameters clearly contribute (along with unresolved [59]Co hfs) in dinuclear systems, dipolar, and possibly, weak exchange couplings. By comparison with spectra from hexaquo-Co(II), the spin concentration of the spectrum from [CoCo(DapE)] suggested 2 mol of EPR-detectable Co(II) per mol of DapE. No signals were observed with $B_0||B_1$ (parallel mode).

DISCUSSION

The emergence of several pathogenic bacterial strains that are resistant to all currently available antibiotics poses a tremendous worldwide health problem (*1−4*). The meso-diaminopimelate (mDAP)/lysine biosynthetic pathway offers several potential anti-bacterial targets that have yet to be explored (*11*, *28*, *29*). DapE, one of the members of this pathway, has been identified in *E. coli*, *H. influenzae*, *Bordetella pertussis*, *Corynebacterium glutamicum*, *H. pylori*, *M. smegmatis*, and *Mycobacterium tuberculosis*, to name a few (*12*, *13*, *15*, *19*, *30*, *31*). Alignment of each of the gene sequences with the structurally characterized dinuclear Zn-(II) hydrolases AAP and GCP$_2$ revealed significant sequence homology, especially in the amino acids functioning as metal ligands (*14*, *16*). However, it should be noted that no catalytically important amino acid residues have been identified for any DapE enzyme. Both AAP and CPG$_2$ possess a (μ-aquo)(μ-carboxylato)dizinc(II) core with one terminal carboxylate and histidine residue bound to each metal ion (Figure 8) (*32*, *33*). Both Zn(II) ions in AAP and CPG$_2$ reside in a distorted tetrahedral coordination geometry. The enzymatic activity of the DapE from *H. influenzae* has recently been shown to be dependent on Zn(II) ions (*14*); therefore, DapEs may belong to the same peptidase family, M28, as AAP and CPG$_2$ (*34*). In an effort to gain insight into the structural and catalytic properties of the active site of DapEs, we have examined the substrate specificity, metal binding properties, and spectroscopic signatures of the Zn(II)- and Co(II)-loaded forms of the DapE from *H. influenzae*.

Similar to AAP, it was shown that the as-purified DapE enzyme contains only one tightly bound Zn(II) ion and exhibits ~80% of its total activity in the presence of one Zn(II) ion. Substitution of Zn(II) with Co(II) provided an enzyme that was hyperactive by ~2× (*14*). We have verified these data and determined the K_m and k_{cat} values for [ZnZn-(DapE)] toward L,L-SDAP (0.73 mM and 140 s^{-1}, respectively). These data are similar to those previously reported for the DapE from both *E. coli* (0.4 mM and 270 s^{-1}) (*19*) and *H. influenzae* (1.3 mM and 200 s^{-1}) (*14*). As is typical for many metallohydrolases, DapE can be activated by a number of divalent metal ions including manganese, nickel, and copper (*23*). These results are similar to those reported

for the *argE*-encoded *N*-acetylornithine deacetylase, a protein involved in arginine biosynthesis that shares a significant amount of sequence homology to DapE (*35*). Interestingly, AAP cannot be activated by Mn(II) (*36*), whereas the leucine aminopeptidase from bovine lens is active in the presence of Mg(II) or Mn(II) (*37*). The fact that DapE is active with such a broad range of metals may be suggestive of its overall importance within the bacterial cell. Even under conditions where zinc may be limiting, cell wall synthesis would not be affected.

On the basis of the fact that DapE can be activated to 80% of its full enzymatic level with one Zn(II) ion, one divalent metal binding site is likely filled preferentially. Therefore, kinetic data for mixed-metal species of DapE were obtained. The observed K_m value for [ZnCo(DapE)] toward L,L-SDAP was significantly lower than that observed for [ZnZn(DapE)] (K_m: 0.26 vs 0.73 mM) suggesting that the second metal ion plays a significant role in both substrate binding and positioning of the nucleophile. Interestingly, [ZnCo(DapE)] is the best catalyst since its catalytic efficiency (k_{cat}/K_m) is 16 800 versus 11 400 mM^{-1} min^{-1} for [ZnZn-(DapE)]. Because DapE is 80% active in the presence of one Zn(II) ion, the first metal ion must function as the catalytic site and deliver the nucleophile during catalytic turnover. The role of the second metal ion is less clear at this time, but it must participate in the binding and positioning of substrate. Moreover, it is apparent based on these data that the transition metal ions bound in the active site of DapE effect both substrate binding and rate-limiting step of catalysis. These data are similar to those observed for AAP (*20, 21*).

The design and synthesis of novel DapE inhibitors requires information regarding substrate specificity. Therefore, the four isomers of SDAP as well as a number of acetylated amino acids were examined as potential substrates (Figure 2). These amino acid derivatives have similar side chains to SDAP and were examined to determine the structural components necessary for substrate binding to the active site of DapE. DapE was not able to hydrolyze the D,D-, L,D-, or D,L-forms of SDAP indicating that L,L-SDAP is the only known biological substrate for DapE enzymes. Moreover, no degradation was observed for any of the acetylated amino acids tested. These data verify the strict substrate specificity of the DapE active site with regard to both functional groups and stereochemistry. These data also suggest that the carboxylate of the succinyl moiety forms an important interaction with the active site of DapE since none of the acetylated amino acids could be hydrolyzed. Alternatively, the acetylated versions of these amino acids may introduce a repulsive interaction because of the methyl group, thus preventing hydrolysis. We therefore examined D,L-succinyl aminopimelate, which only differs from the natural substrate, L,L-SDAP, by the absence of the amine group on the amino acid side chain (Scheme 1). Interestingly, DapE could not hydrolyze this compound implying that the amine provides an important interaction for substrate binding.

Titration of apo-DapE (6 μM) with Zn(II) confirmed that the enzyme was 80% active after the addition of only 1 equiv of Zn(II). Fits of these titration data provided a K_d value for the first metal binding site of 140 nM. Since only one metal ion is bound to the enzyme active site, these K_d values correspond to the microscopic binding constants for the binding of a single metal ion to DapE. This K_d value is similar to K_d values obtained for several other hydrolytic enzymes that contain mixed histidine-carboxylate active sites. For example, the K_d value for the first metal binding site of AAP is 1 nM (*38*), clostridial aminopeptidase exhibits a K_d of 2 μM (*39*), the clostridial AMPP has a reported K_d value of 7 μM (*39*), and the β-lactamase from *Bacillus cereus* has a K_d value of 620 nM (*40*).

To further examine the metal binding properties of DapE, electronic absorption spectra of Co(II)-loaded DapE (1 mM) were recorded. Upon the addition of 1 equiv of Co(II) under anaerobic conditions, three resolvable d—d transitions at 530, 562, and 575 nm (ϵ = 130, 175, and 150 M^{-1} cm^{-1}, respectively) were observed. Ligand-field theory predicts that optical transitions of four-coordinate Co(II) complexes give rise to intense absorptions ($\epsilon > 300$ M^{-1} cm^{-1}) in the higher wavelength region (625 $\pm$ 50 nm) due to a comparatively small ligand-field stabilization energy, while transitions of octahedral Co(II) complexes have very weak absorptions ($\epsilon < 30$ M^{-1} cm^{-1}) at lower wavelengths (525 $\pm$ 50 nm). Five-coordinate Co(II) centers show intermediate features (i.e., moderate absorption intensities ($50 < \epsilon < 250$ M^{-1} cm^{-1})) with several maxima between 525 and 625 nm (*26, 41*). On the basis of the molar absorptivities and d—d absorption maxima of [Co_(DapE)], the first metal binding site is likely pentacoordinate or distorted tetrahedral. However, very little absorbance increase is observed upon the addition of a second equivalent of Co(II) suggesting that the second metal binding site is octahedral. Because the second Co(II) ion is weakly bound to DapE, an equilibrium exists between free and bound Co(II). Therefore, the ϵ value ($\sim$10 M^{-1} cm^{-1}) for the second Co(II) binding event is likely an underestimate of the actual value. Similar results have been reported for Co(II)-substituted AAP (*20, 21, 42*). Fits of two of the absorption maxima provided a K_d value of 300 μM for the second Co-(II) ion at pH 7.5; therefore, the ability of DapE to bind one versus two divalent metal ions is very different (2.2×10^3 times). These data suggest that under physiological conditions in the absence of substrate, the second metal binding site with the larger K_d may only be partially occupied.

Taken with the optical absorption data, the EPR spectra of [Co_(DapE)] support a five-coordinate environment for the first Co(II) binding site. The absence of features due to $M_S = |\pm 3/2\rangle$ transitions render tetrahedral geometry unlikely, while the optical absorption coefficients would be unusually large for octahedral Co(II). The nonzero *E/D* value and relatively small amount of *g*-strain suggest a geometry with less electronic symmetry and less orientational flexibility than is seen for octahedral systems such as hexaquo-Co(II). The lack of resolved hyperfine on the low-field line suggests coordination differences between the catalytic Co(II) ion in DapE and that in AAP. The natures of these differences are not clear but do not involve sulfur coordination. The EPR data for [CoCo(DapE)] suggest that there is little change in the electronic symmetry of the catalytic Co(II) ion upon binding of the second Co(II). These data do, however, indicate substantial line-broadening of the low-field line of the catalytic Co(II) ion and indicate an effect either on the precise coordination geometry of this metal ion or on the electronic properties due to spin—spin interactions between the two Co(II) ions. The spectrum of [CoCo(DapE)] is consistent with five- or six-coordinate Co(II) in the second site with relatively high axial electronic symmetry, although the spectra are not sufficiently well-resolved to determine

the parameters precisely. The spin density accounts for all the added Co(II); therefore, strong exchange coupling appears not to occur between the two cobalt ions.

Since DapE is relatively stable at 40 °C, activation parameters for the ES‡ complex were obtained by examining the hydrolysis of L,L-SDAP as a function of temperature. Construction of an Arrhenius plot from the temperature dependence of DapE activity indicates that the rate-limiting step does not change as a function of temperature (*25*). The activation energy (E_a) for the activated ES‡ complex is 31 kJ/mol for [ZnZn(DapE)]. The observed activation energy is similar to the E_a reported for APP (36.5 kJ/mol), which has a similar activation energy to pronase and both thermolysin and carboxypeptidase A (*43−45*). The enthalpy of activation at 25 °C is 28.5 kJ/mol, while the entropy of activation was found to be −119 J/mol K at 25 °C. The positive enthalpy is indicative of a conformational change upon substrate binding, likely due to the energy of bond formation and breaking during nucleophilic attack on the scissile carbonyl carbon of the substrate. On the other hand, the large negative entropy value suggests that some of the molecular motions are lost upon ES‡ complex formation possibly due to hydrogen bond formation between catalytically important amino acids and the substrate. All of these factors contribute to the large positive free energy of activation.

In conclusion, only L,L-SDAP can be hydrolyzed by DapE suggesting that small molecules that contain some or all of the recognition features of SDAP may function as potent inhibitors of DapE. Studies are underway to determine which substrate features are critical for tight binding of small molecules to DapE and which are not. Moreover, the spectroscopic data presented herein provide the first structural glimpse at the active site metal ions of any DapE enzyme. Electronic absorption and EPR spectra of [Co_(DapE)] and [CoCo(DapE)] suggest that the first Co(II) binding site is five-coordinate, while the second site is octahedral. Combination of the kinetic and spectroscopic data presented herein suggests that the DapE from *H. influenzae* has similar divalent metal binding properties to AAP. Further studies are required to understand the exact binding nature of Co-(II) and other activating divalent metal ions to DapE.

ACKNOWLEDGMENT

REFERENCES

1. Prevention, C. f. D. C. a. (1995) *MMWR Morb. Mortal. Weekly Rep. 44*, 1−13.
2. Howe, R. A., Bowker, K. E., Walsh, T. R., Feest, T. G., and MacGowan, A. P. (1997) *Lancet 351*, 601−602.
3. Levy, S. B. (1998) *Sci. Am. 278*, 46−53.
4. Chin, J. (1996) *New Scientist 152*, 32−35.
5. Henery, C. M. (2000) *C&E News*, 41−58.
6. Miller, J. B. (2000) *The Pharma Century*, pp 52−71.
7. Lesney, M. S., and Tweedy, B. D. (2000) *The Pharma Century*, pp 72−91.
8. Lesney, M. S., and Frey, R. (2000) *The Pharma Century*, pp 110−129.
9. Lesney, M. S., and Frey, R. (2000) *The Pharma Century*, pp 92−109.
10. Nemecek, S. (1997) *Sci. Am. 276*, 38−39.
11. Scapin, G., and Blanchard, J. S. (1998) *Adv. Enzymol. 72*, 279−325.
12. Karita, M., Etterbeek, M. L., Forsyth, M. H., Tummuru, M. R., and Blaser, M. J. (1997) *Infect. Immun. 65*, 4158−4164.
13. Pavelka, M. S., and Jacobs, W. R. (1996) *J. Bacteriol. 178*, 6496−6507.
14. Born, T. L., Zheng, R., and Blanchard, J. S. (1998) *Biochemistry 37*, 10478−10487.
15. Bouvier, J., Richaud, C., Higgins, W., Bögler, O., and Stragier, P. (1992) *J. Bacteriol. 174*, 5265−5271.
16. Makarova, K. S., and Grishin, N. V. (1999) *J. Mol. Biol. 292*, 11−17.
17. D'souza, V. M., and Holz, R. C. (1999) *Biochemistry 38*, 11079−11085.
18. Bergmann, M., and Stein, W. H. (1939) *J. Biol. Chem. 129*, 609−618.
19. Lin, Y., Myhrman, R., Schrag, M. L., and Gelb, M. H. (1988) *J. Biol. Chem. 263*, 1622−1627.
20. Bennett, B., and Holz, R. C. (1997) *J. Am. Chem. Soc. 119*, 1923−1933.
21. Bennett, B., and Holz, R. C. (1997) *Biochemistry 36*, 9837−9846.
22. Griffin, M., Muys, A., Noble, C., Wang, D., Eldershaw, C., Gates, K. E., Burrage, K., and Hanson, G. R. (1999) *Mol. Phys. Rep. 26*, 60.
23. Bennett, B., Antholine, W. E., D'souza, V., Ustynyuk, L., Chen, G., and Holz, R. (2002) *J. Am. Chem. Soc. 124*, 13025−13034.
24. Winzor, D. J., and Sawyer, W. H. (1995) *Quantitative Characterization of Ligand Binding*, Wiley-Liss, New York.
25. Segel, I. H. (1975) *Enzyme Kinetics: Behavior and analysis of rapid equilibrium and steady-state enzyme systems*, 1st ed., John Wiley & Sons, New York.
26. Bertini, I., and Luchinat, C. (1984) *Adv. Inorg. Biochem. 6*, 71−111.
27. D'souza, V. M., Bennett, B., Copik, A. J., and Holz, R. C. (2000) *Biochemistry 39*, 3817−3826.
28. Born, T. L., and Blanchard, J. S. (1999) *Curr. Opin. Chem. Biol. 3*, 607−613.
29. Girodeau, J.-M., Agouridas, C., Masson, M., Pineau, R., and LeGoffic, F. (1986) *J. Med. Chem. 29*, 1023−1030.
30. Fuchs, T. O., Schneider, B., Krumbach, K., Eggeling, L., and Gross, R. (2000) *J. Bacteriol. 182*, 3626−3631.
31. Shaw-Reid, C. A., McCormick, M. M., Sinskey, A. J., and Stephanopoulos, G. (1999) *Appl. Microbiol. Biotechnol. 51*, 325−333.
32. Chevrier, B., Schalk, C., D'Orchymont, H., Rondeau, J.-M., Moras, D., and Tarnus, C. (1994) *Structure 2*, 283−291.
33. Rowsell, S., Pauptit, R. A., Tucker, A. D., Melton, R. G., Blow, D. M., and Brick, P. (1997) *Structure 5*, 337−347.
34. Barrett, A. J., Rawlings, N. D., and Woessner, J. F. (1998) *Handbook of Proteolytic Enzymes*, pp 1−1666, Academic Press, London.
35. Javid-Majd, F., and Blanchard, J. S. (2000) *Biochemistry 39*, 1285−1293.
36. Prescott, J. M., Wagner, F. W., Holmquist, B., and Vallee, B. L. (1983) *Biochem. Biophys. Res. Commun. 114*, 646−652.
37. Allen, M. P., Yamada, A. H., and Carpenter, F. H. (1983) *Biochemistry 22*, 3778−3783.
38. Prescott, J. M., and Wilkes, S. H. (1976) *Methods Enzymol. 45*, 530−543.
39. Fleminger, G., and Yaron, A. (1984) *Biochim. Biophys. Acta 789*, 245−256.
40. de Seny, D., Heinz, U., Wommer, S., Kiefer, M., Meyer-Klaucke, W., Galleni, M., Frere, J.-M., Bauer, R., and Adolph, H.-W. (2001) *J. Biol. Chem. 276*, 45065−45078.
41. Horrocks, W., DeW., I., Jr., Holmqust, B., and Thompson, J. S. (1980) *J. Inorg. Chem. 12*, 131−141.
42. Prescott, J. M., Wagner, F. W., Holmquist, B., and Vallee, B. L. (1985) *Biochemistry 24*, 5350−5356.
43. Lumry, R., Smith, E. L., and Glantz, R. R. (1951) *J. Am. Chem. Soc. 73*, 4330−4340.
44. Kunugi, S., Hirohara, H., and Ise, N. (1982) *Eur. J. Biochem. 124*, 157−163.
45. Wu, C.-H., and Lin, W.-Y. (1995) *J. Inorg. Biochem. 57*, 79−89.